EasyChair Preprint

№ 6929

Thermal and emission characteristics of liquid Fuel flameless combustion in a forward flow combustion chamber

Mohammed Bashir Abdulrahman, Mazlan Abdul Wahid, Ali Asmayou, Adam Kasani, Mohd Fairus Mohd Yasin and Md. Mizanur Rahman

October 26, 2021

Thermal and Emissions Characteristics of Liquid Fuel Flameless Combustion in a Forward Flow Combustion Chamber

Mohammed Bashir Abdulrahman[1, 2, a], Mazlan Abdul Wahid[1, b], Ali Houssein Asmayou[1, c], Adam Kasani[1, d], Mohd Fairus Mohd Yasin[1, e], Md Mizanur Rahman[1, f]

[1] *High-Speed Reacting Flow Laboratory, Faculty of Engineering, School of Mechanical Engineering, Universiti Teknologi Malaysia, 81310 UTM Skudai, Johor, Malaysia.*
[2] *Department of Mechanical Engineering, Federal Polytechnic Mubi, Adamawa State, Nigeria.*

[a)]Corresponding author: mobash2007@gmail.com
[b)] mazlan@utm.my
[c)]alihasmayou@gmail.com
[d)]adamkasani@gmail.com
[e)]mohdfairus@mail.fkm.utm.my
[f)] mizanur@mail.fkm.utm.my

Abstract. This paper presents the experimental results of liquid fuel flameless combustor for various heat inputs of 10, 12, 14, 16, 18, 20, and 21 kW. The visual observations and temperature profile in the reaction zone and the NOx and CO gasses at the outlet are used to evaluate the performance of the flameless combustor. Fuel and air are injected at ambient conditions. The tangential air inlets acted as swirl generators to improve the internal recirculation rates and residence time and increase the dilution of reactants entering the reaction zone, resulting in flameless combustion. Ethanol is injected symmetrically and axially, while air is injected tangentially through 12 nozzles along the entire length of the combustion chamber. The results showed that by distributing the tangential air inlets along the entire combustion chamber length, the overall swirl strength was reduced by distributing the swirl generators evenly along the entire length of the combustion chamber. This resulted in good combustion performance in flameless combustion mode with low peak temperature in the reaction zone. It is assumed that the uniform temperature distribution in the furnace is the cause of the reduction of NOx to 3.6 ppm and CO to 15 ppm at $\Phi = 0.9$.

INTRODUCTION

The combustion of fossil fuels has been the major energy source worldwide and is believed to continue to do so for another few more decades. Burning it traditionally in industrial heating furnaces and electricity generation has tremendous effects on the environment, ecosystem, and human body due to high pollutants emission, especially nitrogen oxides (NOx) [1]. Due to these effects and to cope with the stringent environmental protection regulations, clean and efficient combustion techniques are constantly explored. Among these, flameless combustion is considered an attractive technique because it suppresses pollutant emissions without compromising thermal efficiency and produces a uniform temperature distribution in the reaction chamber. These interesting combustion features are achieved through enhanced internal recirculation of the flue gases, which results in dilution and preheating of the fresh reactants. In this way, NOx formation by the thermal route and CO emissions are suppressed by this process.[2–4]. The reaction zone of the flameless mode glows with an invisible flame throughout the volume of the furnace [5–7]. To achieve a flameless combustion, the combustor chamber must be first preheated above the auto ignition temperature of the fuel in question and sufficient combustion products must enter the reaction zone [8, 9]. This novel combustion technique can be performed with high [10], and low [11] preheated combustion air [12, 13] as well as air at ambient temperature [14].

Flameless combustion with gaseous fuels has been thoroughly investigated for various configurations and flow fields [15–18] because the reactants of the mix easily. [19]. Liquid fuel combustion, on the other hand, requires involves complex processes in a short time, such as fuel injection, atomization, droplet evaporation and perfect mixing of reactants, followed by combustion [20–22]. In conventional combustion, flame stabilizes near the fuel injection and forms a high temperature region at the nozzle exit, resulting in vaporation and combustion the fuel droplets [23]. Since a higher percentage of combustion systems use liquid fuels, it is imperative to develop liquid fuels flameless combustors. Previous studies on flameless combustion using liquid fuels as reported in the literature [5, 22, 24–27], mostly considered small and complex structures, with only four tangential air inlet ports located near the fuel nozzle [27]. The burners were often seen to combine co-axial air inlets and with swirling fuel injector

nozzles [28]. Some of the burners used preheated combustion air [11] while others used pre-heated fuel [29] in the combustion reaction. However, the influence of distributed tangential air inlets (air swirling) across the entire combustor length and direct fuel injection on combustion characteristics has not been discussed in the literature. Therefore, in this paper, based on air swirling combustion, we proposed a novel and unique tangential air injection configuration (**FIGURE 1**) to improve combustion quality by achieving sufficient recirculation of the hot combustion products inside the combustor in a broad range of equivalence ratios (Φ). The experimental studies are conducted to demonstrate the sustainability of the flameless combustion regime in the proposed furnace and evaluate its performance in terms of temperature distribution and uniformity, pollutant emissions, and visualization of the reaction zone.

EXPERIMENTAL METHODOLOGY

Experimental Setup

FIGURE 1a shows the isometric view of the rig, and **FIGURE 1b** is the schematic of the instrumented rig. The combustor is placed vertically on a test stand, as shown in **FIGURE 2**. Combustion air is supplied from the compressor and the air flow rate is manually controlled using flowmeters. Liquid fuel is injected axially through a direct nozzle to the reaction zone from a pressurized tank with the aid of high pressure N_2 gas. The fuel nozzle is mounted symmetrically at the center of the combustor. During the warm-up stage, air is supplied to both axial and tangential inlets. Whereas in flameless, only the tangential inlets were in used. The 12 tangential air inlets (swirlers) are evenly spread across the combustor length and circumference; to improve the mixing process and improve recirculation rate of the hot combustion products. The combustor is tested under seven different thermal inputs of 10, 12, 14, 16, 18, 20, and 21 kW with fixed combustion air supply of 0.566g/s. Equivalence ratios (Φ) were calculated using equation 1. The combustor is operated with ethanol as liquid fuel at 9bar injection pressure. The furnace combustion chamber is well insulated with a 65 mm thick high-temperature ceramic fiber layer that allows only about 10% heat loss through the outside wall of the combustor. As a result, the establishment and stability of the flameless regime from a cold state until steady-state operation can be achieved in good time

$$\Phi = \frac{\left(\frac{\mathrm{A}}{\mathrm{F}}\right)\mathrm{Stoic}}{\left(\frac{\mathrm{A}}{\mathrm{F}}\right)\mathrm{Actual}} \tag{1}$$

Where $\left(\frac{A}{F}\right)Stoic = \frac{\dot{m_{air}}}{\dot{m_{fuel}}} = \frac{4.76aMW_{air}}{MW_{fuel}}$ and $\left(\frac{A}{F}\right)Actual = \frac{\dot{m_{air}}}{\dot{m_{fuel}}}$

Experimental Procedure and Instruments

Initially, the furnace is ignited with a premixed LPG-air mixture at stoichiometric conditions operated conventionally for about an hour to warm up the combustor. The stable flame gradually shifted to a flameless state by slowly closing the axial air inlets and topping up the tangential inlets to maintain the stoichiometric condition. After which, liquid fuel is injected at 9 bar while closing the LPG supply [30]. The combustor is prepared with different instrumentation systems for data acquisition, as shown in **FIGURE 1b**. The temperature measurements were collected by a laptop through thermocouples that connected to a TC-08 data logger. A TESTO 350 gas analyzer is used to measure gas composition (O_2, CO, NO_x, NO, and NO_2) inside the exhaust pipe every second for at least 1 minute. The images of the reaction zone are captured HUAWEI nova 3i with 2340 by1080 resolution.

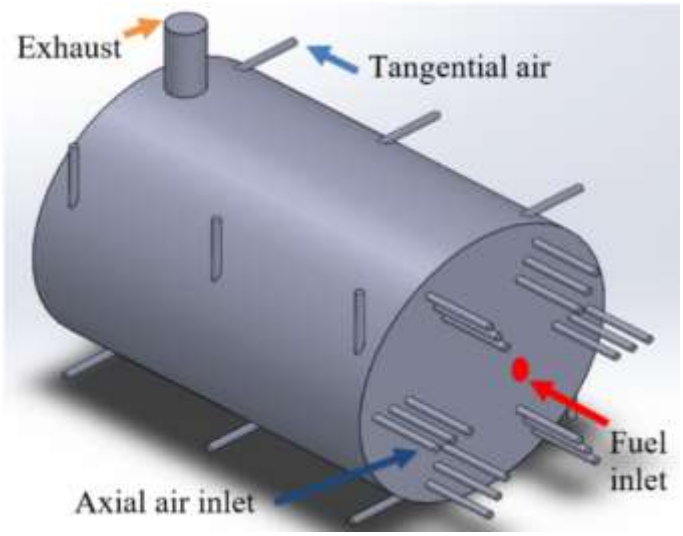

(a)

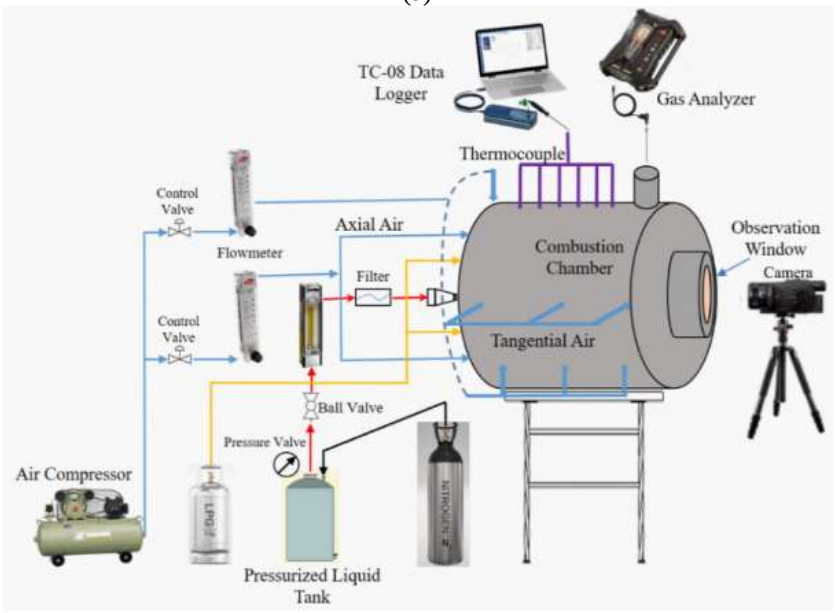

(b)

FIGURE 1. Isometric view (a) and the schematic of the instrumented rig (b). In a forward flow configuration, the fuel inlet and exhaust pipe are positioned opposite sides but flowing in the same direction

FIGURE 2. Experimental setup

RESULTS AND DISCUSSIONS

Transition from Conventional to MILD Combustion

FIGURE 3 presents a sequence of images of the combustion reaction transformation from conventional flame into flameless regime. A well-defined flame zone is observed in **FIGURE 3a**. The gradual disappearance of flame in the combustion chamber refers to the transitional state (**FIGURE 3b**) and flameless mode is observed in **FIGURE 3c**. The disappearance of flame was evidenced by the sudden decrease in furnace reference temperature, as shown in **FIGURE 4**. The **FIGURE 4** shows the average temperature along the furnace centreline. The transition from a conventional flame to flameless mode occurred when the combustion chamber temperature drops from about 930ºC to around 830ºC. At this point, LPG injection was gradually reduced while ethanol supply was gradually increased.

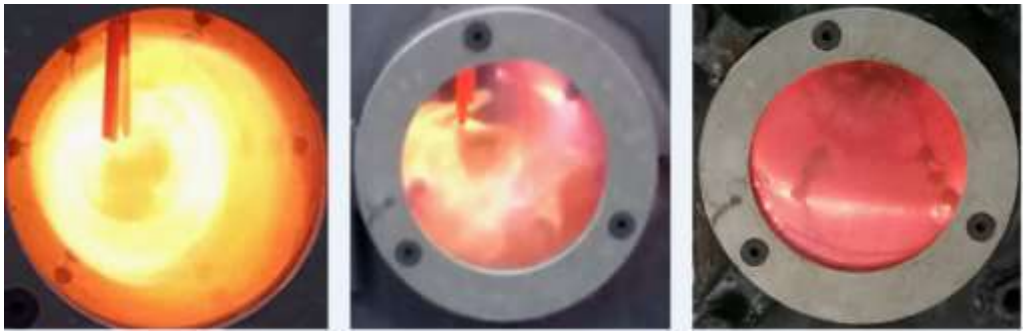

(a) (b) (c)

FIGURE 3. (a) Conventional combustion, (b) Transitional combustion, (c) Flameless combustion.

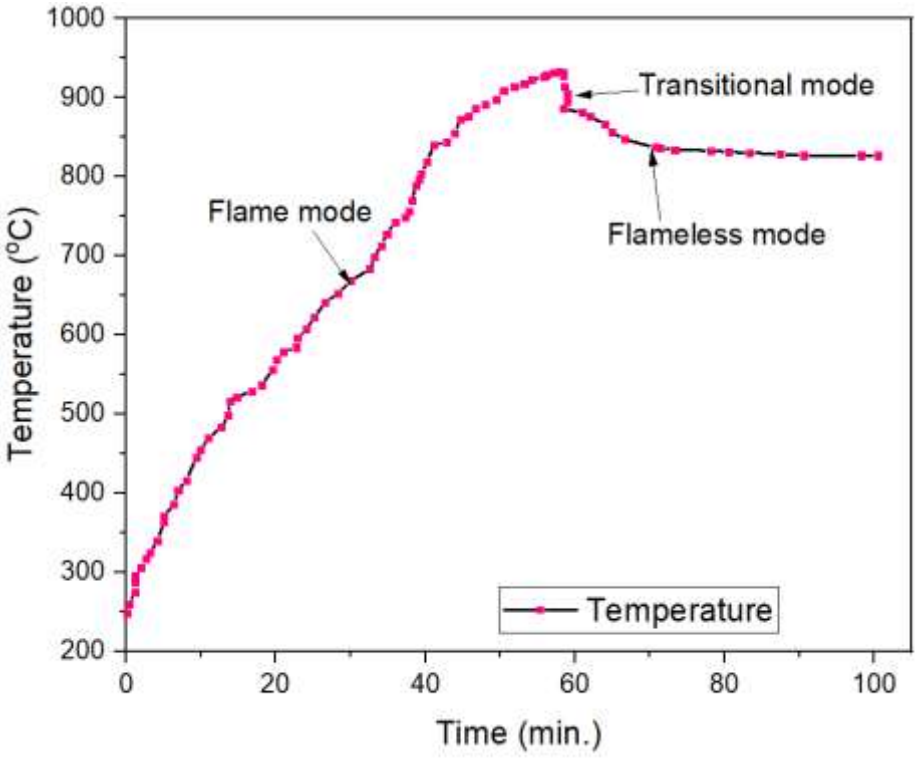

FIGURE 4. Variation of combustion chamber temperature with time.

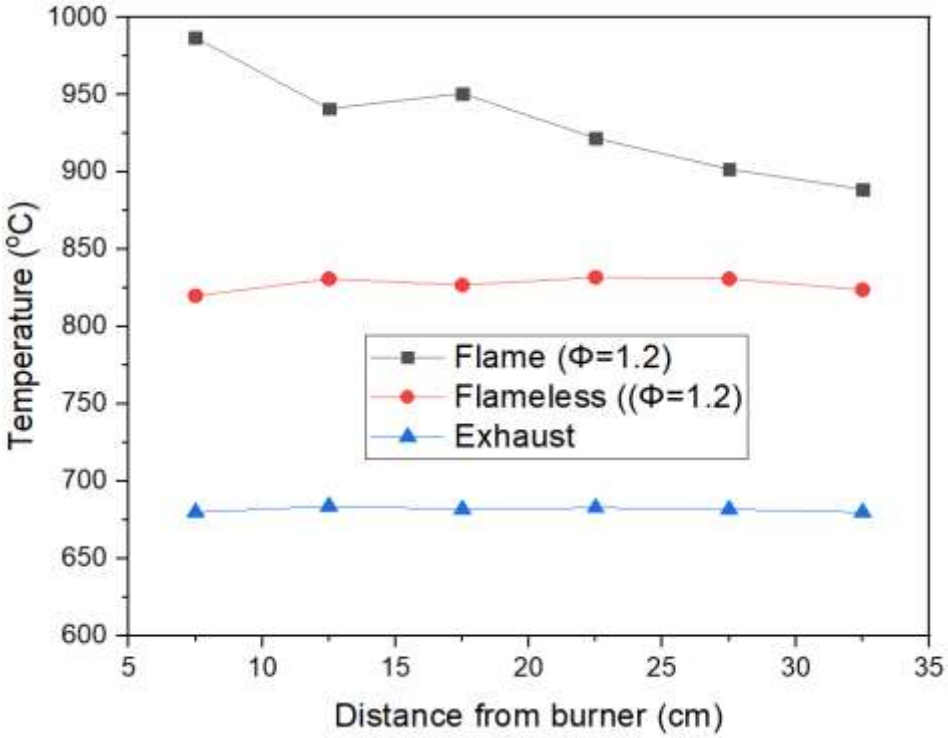

FIGURE 5. Temperature variation along the central furnace axis.

FIGURE 5 further compares the temperature distribution along the furnace axis in flame and flameless modes at Φ=1.2. Temperature field reduction was observed in a flameless state, which is equivalent to about 11%. The temperature is lower and uniform in flameless mode than in traditional mode. The uniform and low-temperature gradient throughout the furnace are essential and desirable characteristics of flameless combustion. The exhaust temperature is almost constant, around 680°C [31]. This temperature is about 18% less concerning the flameless temperature in the furnace.

Temperature Profiles

FIGURE 6a shows the temperature distribution inside the reaction chamber for the range of thermal inputs in flameless regimes. Generally, the mean thermal fields are quite uniform, as the maximum temperature differences between the upstream and downstream for all the thermal inputs are less than 21°C. However, it is evident from **FIGURE 6&b** that as the fuel-air mixture decreased, the overall combustion temperature also reduced. For an instant, at thermal input of 21 KW, **FIGURE 6a** recorded the highest thermal field (831°C) and 10 kW the least (760°C). Thermodynamically, the combustion temperature increases as the fuel to air mixture increased due to the higher heat released by the extra energy in the mix and vice-versa. The temperature drop observed near the furnace inlet in **FIGURE 6a**, is believed to be caused by the effect of dilution due to the injection of fresh fuel at room temperature.

Moreover, the drop in temperatures at the combustor exit is caused by heat lost from exhaust gas exiting the combustion chamber and through the observation window [32]. The peak temperatures in the flameless mode are far less than that in flame mode (**FIGURE 6b**) and farther less than the thermal NO_x formation temperature (1200°C) [33]. The low peak temperature in flameless mode causes a significant reduction of NO_x formation.

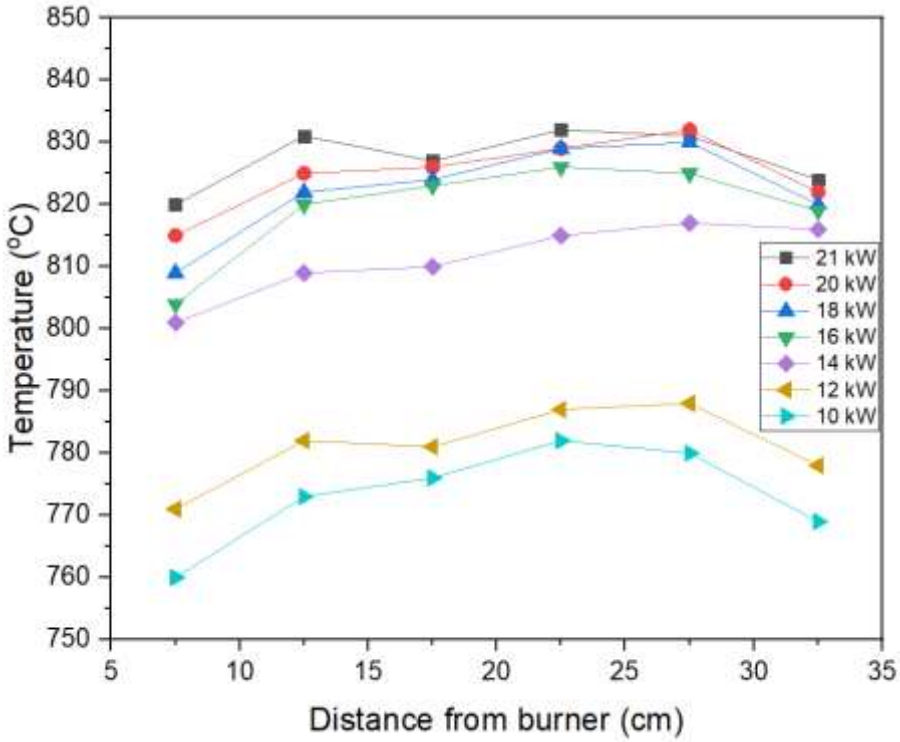

(a)

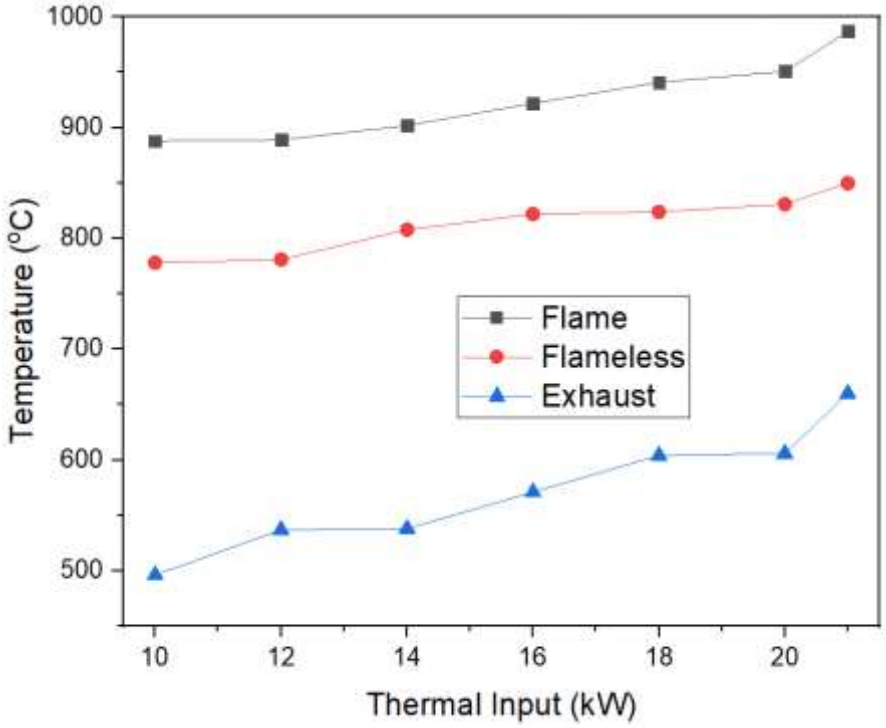

(b)

FIGURE 6. Temperature profile along the central furnace axis for ethanol flameless combustion against a distance from the burner and thermal input.

The proportionality of the heat load to furnace temperatures (flame, flameless, and exhaust) is further demonstrated in **FIGURE 6b**. The furnace temperatures drop as thermal input decreases until the lean blowout due to heat loss in warming up the excess air. The extra air leads to lean extinction as witnessed in 12 kW (Φ=0.7) and 10 kW (Φ =0.6). This is because, near the lean operational limit, the furnace is susceptible to combustion instabilities. Heat loss from the furnace is quantifiable by measuring the exhaust temperature. The estimation of heat losses gives the operational behavior of the furnace. The result presented in **FIGURE 6b**

reveals that the heat losses between the heat input and exhaust are less than 18%.

Pollutants Emission

To examine the effects of Φ in respect to thermal inputs on flameless combustion, the resulting NO_x, CO and O_2 were measured for the range of Φ at the combustor exit. The effect of Φ on NO_x is shown in **FIGURE 7a**. Generally, low NO_x levels of less than 9 ppm were discerned. The drop in NO_x emission in flameless mode is attributed to fewer hot spots in the reaction zone, which inhibits NO_x formation via the thermal mechanism. The NO_x starts to increase sharply when the equivalence ratio (Φ) approaches stoichiometric condition, specifically at Φ of 0.9. The sharp rise is due to the increase in furnace temperature due to the rise in thermal input, which conforms with [34].

Conversely, the NO_x level increases towards the lean extinction limit due to incomplete combustion. The lowest NO_x levels of about 3.6 ppm were recorded at Φ of 0.9 and a maximum of 7 ppm at Φ of 1.2. Furthermore, the combustor's highly uniform temperature and thermal field below 950°C guaranteed the very low NO_x level produced.

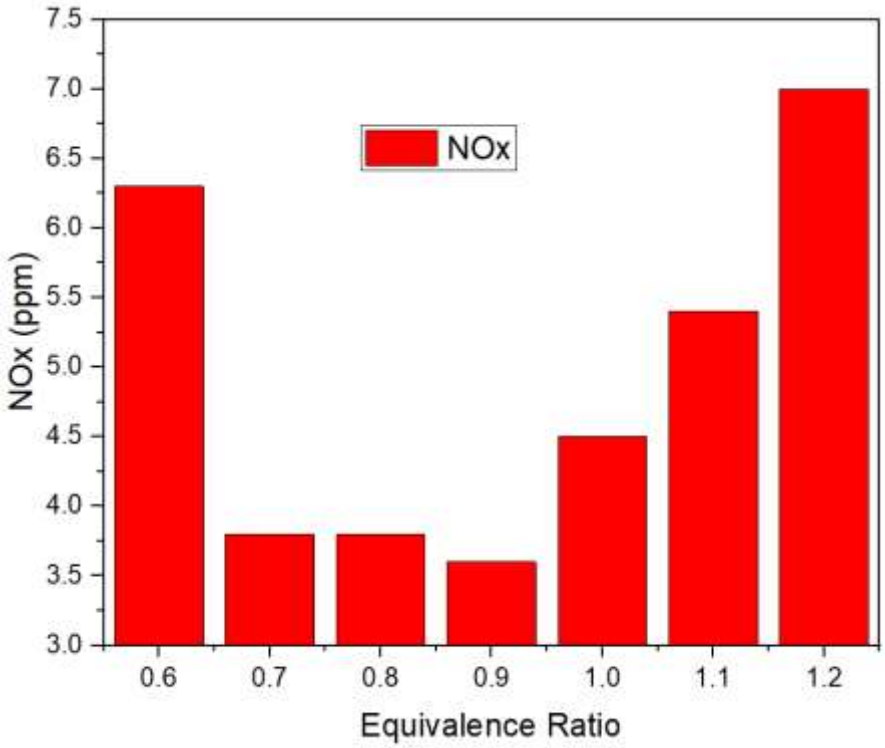

(a)

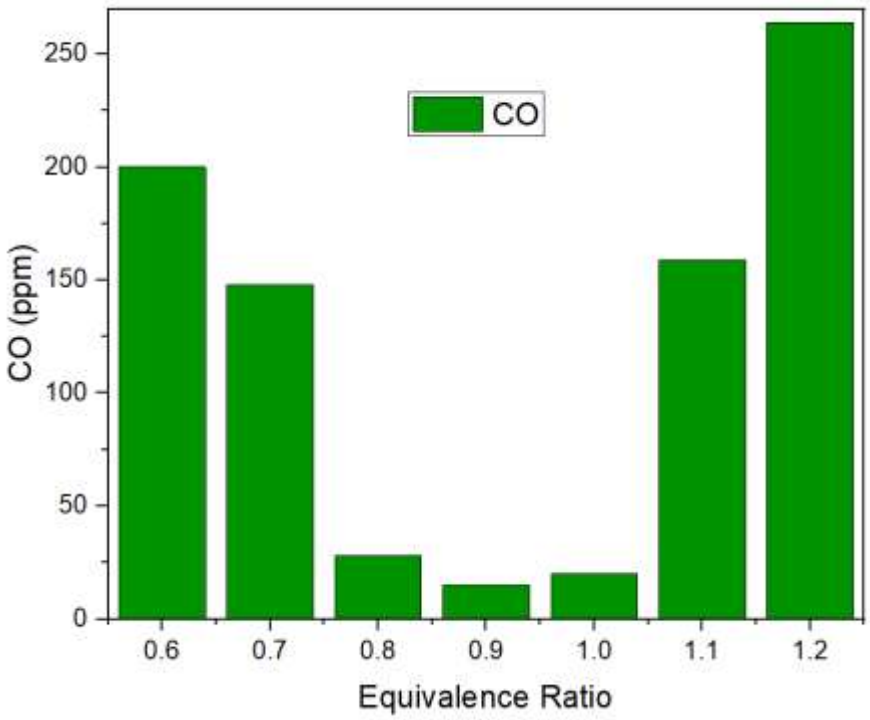

(b)

FIGURE 7. NO_x and CO emissions in flameless combustion conditions for ethanol as a function of Φ at 3% O_2 by volume.

FIGURE 7b shows the measured CO values against the equivalence ratio. It can be seen that the lowest CO levels were recorded around stoichiometry. The level of CO gas emission can be seen to reduce up until Φ=0.9. This can be attributed to the deficiency of O_2 concentration and dissociation of CO_2 being exalted [35]. The CO levels drastically increased from Φ =0.8 toward excess lean. This is due to incomplete combustion at lean extinction. The least CO emission of 15 ppm was recorded at Φ=0.9 and the highest of 264 ppm at Φ=1.2. Favorable operating conditions were found to be at Φ near stoichiometry for both NO_x and CO emission levels and increased significantly at higher Φ. This may be as a result of lower residence time associated with higher heat release intensity and lower Φ, due to incomplete combustion.

CONCLUSIONS

This study experimentally investigated liquid fuel flameless combustion characteristics for a range of thermal inputs in a forward flow cylindrical combustor. The results demonstrate that flameless combustion of liquid fuel is sustainable over a wide range of equivalence ratios (Φ= 0.6-1.2) in terms of thermal inputs, with the influence of distributed tangential air inlets across the entire combustor length. However, it is more sustainable at stoichiometry with averagely low peak temperature and uniformly distributed heat energy indicated by the uniform temperature profile throughout the furnace volume. The Lowest emissions of NO_x and CO were 3.6 ppm and 15 ppm, respectively, recorded at Φ= 0.9. Therefore, the optimal flameless combustion condition for the present combustor is at an equivalence ratio of 0.9. It was further revealed that swirl (tangential air inlets) is an essential parameter in liquid fuel combustion for better mixing because liquid fuel is more difficult to mix with the combustion air and burn compared to gaseous fuels.

ACKNOWLEDGMENTS

The first author wishes to thank the Nigerian government for the scholarship award through the Tertiary Education Trust Fund (TETFUND). Our heartfelt gratitude goes to the UTM High Impact Research Grant Vote 09G05. And our highest appreciation goes to the members of HiREF laboratory, Universiti Teknologi Malaysia.

REFERENCE

1. Z.X. Chen, N.A.K. Doan, X.J. Lv, N. Swaminathan, G. Ceriello, G. Sorrentino, A. Cavaliere, Numerical Study of a Cyclonic Combustor under Moderate or Intense Low-Oxygen Dilution Conditions Using Non-

adiabatic Tabulated Chemistry, Energy and Fuels. 32 (2018) 10256–10265.
2. J.A. Wünning, J.G. Wünning, Flameless Oxidation to Reduce Thermal No-Formation, Prog. Energy Combust. Sci. 23 (1997) 81–94.
3. G. Ceriello, G. Sorrentino, A. Cavaliere, P. Sabia, M. de Joannon, R. Ragucci, The role of dilution level and canonical configuration in the modeling of MILD combustion systems with internal recirculation, Fuel. 264 (2020).
4. S.E. Hosseini, M.A. Wahid, A.A.A. Abuelnuor, The Role of Exhaust Gas Recirculation in Flameless Combustion, Appl. Mech. Mater. 388 (2013) 262–267.
5. S. Garnayak, M.R. Vanteru, S.K. Dash, Liquid Fuel Combustion with Extremely Diluted Oxidizer in High Swirl Flows at High Pressure, in: Proc. 2nd Natl. Aero Propuls. Conf., Kharagpur, West Bengal NAPC2018-022, 2018.
6. V.M. Reddy, S. Kumar, Development of High Intensity low Emission Combustor for Achieving Flameless Combustion of Liquid Fuels, Propuls. Power Res. 2 (2013) 139–147.
7. M. Ferrarotti, D. Lupant, A. Parente, Analysis of a 20 kW flameless furnace fired with natural gas, Energy Procedia. 120 (2017) 104–111.
8. J.S. Feser, S. Karyeyen, A.K. Gupta, Flowfield impact on distributed combustion in a swirl assisted burner, Fuel. 263 (2020) 116643.
9. A. Cavaliere, M. De Joannon, Mild combustion, 2004. https://doi.org/10.1016/j.pecs.2004.02.003.
10. M. Katsuki, T. Hasegawa, The science and technology of combustion in highly preheated air, Symp. Combust. 27 (1998) 3135–3146.
11. Y. Tu, K. Su, H. Liu, Z. Wang, Y. Xie, C. Zheng, W. Li, MILD combustion of natural gas using low preheating temperature air in an industrial furnace, Fuel Process. Technol. 156 (2017) 72–81..
12. G. Sorrentino, P. Sabia, M. de Joannon, P. Bozza, R. Ragucci, Influence of preheating and thermal power on cyclonic burner characteristics under mild combustion, Fuel. 233 (2018) 207–214.
13. R. Weber, J. P. Smart, On the (MILD) combustion of gaseous, liquid, and solid fuels in high temperature preheated air, Proc. Combust. Inst. 30 (2005) 2623–2629.
14. A. Kasani, Combustion characteristics of a direct injection liquid Fueled flameless combustor with ultra-high swirl flow configuration, n.d.
15. S. Sharma, P. Singh, A. Gupta, A. Chowdhury, B. Khandelwal, S. Kumar, Distributed combustion mode in a can-type gas turbine combustor – A numerical and experimental study, Appl. Energy. 277 (2020) 115573.
16. R. Lückerath, W. Meier, M. Aigner, FLOX® combustion at high pressure with different fuel compositions, J. Eng. Gas Turbines Power. 130 (2008) 1–7..
17. G. Sorrentino, P. Sabia, P. Bozza, R. Ragucci, Impact of external operating parameters on the performance of a cyclonic burner with high level of internal recirculation under MILD combustion conditions, Energy. 137 (2017) 1167–1174.
18. P. Sabia, G. Sorrentino, P. Bozza, G. Ceriello, R. Ragucci, M. De Joannon, Fuel and thermal load flexibility of a MILD burner, Proc. Combust. Inst. 37 (2019) 4547–4554.
19. F. Xing, A. Kumar, Y. Huang, S. Chan, C. Ruan, S. Gu, X. Fan, Flameless Combustion with Liquid Fuel: A Review Focusing on Fundamentals and Gas Turbine Application, Appl. Energy. 193 (2017) 28–51.
20. M.A. Khan, H. Gadgil, S. Kumar, Influence of liquid properties on atomization characteristics of flow-blurring injector at ultra-low flow rates, Energy. 171 (2019) 1–13.
21. C.G. de Azevedo, J.C. de Andrade, F. de Souza Costa, Flameless compact combustion system for burning hydrous ethanol, Energy. 89 (2015) 158–167.
22. V.M. Reddy, A. Katoch, W.L. Roberts, S. Kumar, Experimental and Numerical Analysis for High Intensity Swirl Based Ultra-Low Emission Flameless Combustor Operating With Liquid Fuels, Proc. Combust. Inst. 35 (2015) 3581–3589.
23. C.L. Cha, H.Y. Lee, S.S. Hwang, The effect of diluted hot oxidant and fuel on NO formation in oxy-fuel flameless combustion using opposite jet †, 33 (2019) 3709–3716. https://doi.org/10.1007/s12206-019-0712-4.
24. H. Luhmann, F.C. Maldonado, R. Spörl, G. Scheffknecht, Flameless Oxidation of Liquid Fuel Oil in a Reverse-Flow Cooled Combustion Chamber, Energy Procedia. 120 (2017) 222–229.
25. V.M. Reddy, D. Sawant, D. Trivedi, S. Kumar, Studies on a Liquid Fuel Based Two Stage Flameless Combustor, Proc. Combust. Inst. 34 (2013) 3319–3326. [26] M. Derudi, R. Rota, 110th Anniversary: MILD Combustion of Liquid Hydrocarbon-Alcohol Blends, Ind. Eng. Chem. Res. 58 (2019) 15061–15068.

27. S. Sharma, Effect of CO 2 / N 2 Dilution on Characteristics of Liquid Fuel Combustion in Flameless Combustion Mode, Combust. Sci. Technol. (2020).
28. G.G. Szegö, B.B. Dally, G.J. Nathan, Operational characteristics of a parallel jet MILD combustion burner

system, Combust. Flame. 156 (2009) 429–438..
29. J. Ye, P.R. Medwell, E. Varea, S. Kruse, B.B. Dally, H.G. Pitsch, An Experimental Study on MILD Combustion of Prevaporised Liquid Fuels, Appl. Energy. 151 (2015) 93–101.
30. S. Sharma, H. Pingulkar, A. Chowdhury, S. Kumar, A New Emission Reduction Approach in MILD Combustion through Asymmetric Fuel Injection, Combust. Flame. 193 (2018) 61–75..
31. S.E. Hosseini, M.A. Wahid, Biogas Utilization: Experimental Investigation on Biogas Flameless Combustion in Lab-scale Furnace, Energy Convers. Manag. 74 (2013) 426–432.
32. K. Adam, A. Mazlan, M. Amri, A. Saat, F. Mohd, On The Effects of Fuel Inlet Configurations and Equivalence Ratio to the Pre-Heating Stage Of a Liquid Fuelled Flameless Swirl Combustor, in: AIP Conf. Proc., 2019: p. 020040..
33. A.A.A. Abuelnuor, M.A. Wahid, A. Saat, M. Osman, Characterization of a low NOx flameless combustion burner using natural gas, J. Teknol. (Sciences Eng. 66 (2014) 121–125.
34. S. Sharma, A. Chowdhury, S. Kumar, A Novel Air Injection Scheme to Achieve MILD Combustion in a Can-Type Gas Turbine Combustor, Energy. 194 (2020) 116819.
35. V.K. Arghode, A.K. Gupta, Effect of flow field for colorless distributed combustion (CDC) for gas turbine combustion, Appl. Energy. 87 (2010) 1631–1640.